Process Biochemistry 162 (2026) 32–42

Contents lists available at ScienceDirect

Process Biochemistry

journal homepage: www.elsevier.com/locate/procbio

Boosting *Arthrospira platensis* metabolism during biogas upgrading via carbon coated iron-based nanoparticle addition

Chrysa Anagnostopoulou [a,c,d], Laura Vargas-Estrada [a,b], Panagiotis G. Kougias [c], Raúl Muñoz [a,b,*]

[a] Institute of Sustainable Processes, University of Valladolid, C/Dr. Mergelina s/n., Valladolid 47011, Spain
[b] Department of Chemical Engineering and Environmental Technology, University of Valladolid, C/Dr. Mergelina s/n., Valladolid 47011, Spain
[c] Soil and Water Resources Institute, Hellenic Agricultural Organisation DIMITRA, Thermi, Thessaloniki, 57001, Greece
[d] Laboratory of Food Chemistry and Biochemistry, Department of Food Science and Technology, School of Agriculture, Faculty of Agriculture, Forestry and Natural Environment, Aristotle University of Thessaloniki (AUTH), Thessaloniki 54124, Greece

ARTICLE INFO

Keywords:
Arthrospira platensis
Biogas upgrading
Carbon-coated iron nanoparticles
CO_2 consumption
Phycocyanin production

ABSTRACT

Carbon-coated iron-based nanoparticles have demonstrated a significant potential to enhance the performance of biological processes, particularly microalgal cultivation. In this study, the effect of two types of commercially available iron-based nanoparticles, namely CALPECH and SMALLOPS, was evaluated on *Arthrospira platensis* metabolism during biogas upgrading in batch cultures. Both nanoparticles enhanced CO_2 capture, O_2 production, cyanobacterial growth and phycocyanin synthesis across all tested concentrations. However, the highest phycocyanin content (180 $mg{\cdot}g^{-1}$) was reached by the addition of CALPECH nanoparticles at 100 $mg{\cdot}L^{-1}$. Further experiments under stress conditions, including increased light intensity (300 and 600 $\mu mol{\cdot}m^{-2}{\cdot}s^{-1}$) and salinity (0.1–0.5 M NaCl) confirmed the beneficial effects of CALPECH. At 600 $\mu mol{\cdot}m^{-2}{\cdot}s^{-1}$ CALPECH nanoparticles enhanced biomass productivity and increased CO_2 capture by 33 % while maintaining phycocyanin content at 178 $mg{\cdot}g^{-1}$. Moreover, the addition of 100 $mg{\cdot}L^{-1}$ of CALPECH nanoparticles at 0.1 M NaCl slightly improved biogas upgrading performance and increased phycocyanin content to 192.7 $mg{\cdot}g^{-1}$. In this context, increasing salinity to 0.5 M caused stress in *Arthrospira platensis* cells, reducing photosynthetic efficiency regardless of nanoparticle addition. These outcomes highlight the potential of carbon-coated iron-based nanoparticles to improve *Arthrospira platensis* growth and pigment production, which would ultimately increase the techno-economic feasibility of photosynthetic biogas upgrading.

1. Introduction

Biomethane is emerging as an important alternative to fossil fuels, playing a key role in reducing greenhouse gas emissions, thereby supporting efforts to mitigate climate change, and promoting strategic energy autonomy. Biomethane can be obtained by removing CO_2 and other impurities from biogas using different physicochemical and biological upgrading technologies [1,2].

Physicochemical upgrading technologies are commonly employed at a commercial scale, despite requiring high energy demand and incurring significant operational costs. In addition, the separated CO_2 from biogas is typically released into the atmosphere, increasing environmental concerns and wasting a valuable carbon source [3,4]. In this context, biotechnologies, particularly photosynthetic processes based on microalgae, have attracted growing attention in the field of biogas upgrading. These biological systems offer a cost-effective solution for removing both CO_2 and H_2S, while minimizing environmental impacts [5].

Microalgae are capable of capturing CO_2 from biogas and converting it into biomass and valuable compounds, enhancing the techno-economic feasibility of the overall process [6]. Algae species, such as *Chlorella* and *Arthrospira*, are commonly employed in photosynthetic biogas upgrading due to their tolerance to high CO_2 levels (up to 50 % (v/v)) and their high biomass productivities ranging between 0.3 and 0.6 $g{\cdot}L^{-1}{\cdot}d^{-1}$ depending on operational and environmental conditions. During photosynthetic biogas upgrading, up to 98.6 % of CO_2 can be removed, resulting in residual CO_2 concentrations of 2–6 % in upgraded biomethane at pilot and demo scale, thereby boosting the biomethane

* Corresponding author at: Institute of Sustainable Processes, University of Valladolid, C/Dr. Mergelina s/n., Valladolid 47011, Spain.
E-mail address: raul.munoz.torre@uva.es (R. Muñoz).

https://doi.org/10.1016/j.procbio.2026.01.004
Received 25 August 2025; Received in revised form 23 October 2025; Accepted 8 January 2026
Available online 12 January 2026

content above 90 % [2,5,7,8]. However, the high sensitivity of microalgal metabolism to adverse cultivation conditions, such as excessive light intensity, high salinity, pH fluctuations, alkalinity, and insufficient CO_2 transfer into the culture broth, can significantly decrease photosynthetic efficiency and biogas upgrading performance [9–11].

Currently, the integration of nanotechnology into biological systems, particularly via NPs supplementation, has emerged as an effective strategy to enhance processes such as anaerobic digestion and microalgae metabolism [12,13]. NPs have demonstrated multiple beneficial effects on microalgae cultures, including improved CO_2 fixation, enhanced light utilization and increased synthesis of high-value macromolecules. Recent studies have reported that adding zero-valent iron-based NPs improved photosynthetic biogas upgrading by promoting the growth of *Chlorella* species, achieving biomass concentrations above 3 g VSS·L^{-1} and biomass productivities up to 75 g·m^{-2}·d^{-1} in pilot lab-scale systems [14,15]. Moreover, Giannelli and Torzillo [16] showed that the addition of SiO_2 NPs increased the light distribution in *Chlamydomonas reinhardtii* cultures, resulting in a 23 % increase in chlorophyll a content. In this context, employing high-value microalgae such as *Arthrospira platensis* (*A. platensis*) in biogas upgrading represents a promising approach to improve the economic feasibility of biomethane production. Thus, the rising demand for natural and sustainable pigments has positioned the phycocyanin (C-PC) market at USD 185.2 million in 2024, with projections reaching USD 276.4 million by 2030 [17]. Additionally, *A. platensis* exhibits high biomass productivities (0.2–0.6 g· L^{-1} d^{-1}), tolerance to alkaline environments and elevated C-PC yields of up ≈ 200 mg·g^{-1}, positioning this microalga as an attractive candidate for photobiorefinery-based biogas upgrading [8,18].

This study investigated, for the first time, the effect of two distinct carbon-coated iron-based NPs on the growth and phycocyanin production of the cyanobacterium *A. platensis* during batch biogas upgrading assays. The concentration of the most effective NP was further optimized to maximize *A. platensis* growth and pigment synthesis. Finally, to evaluate the potential of the optimal NPs dosage under stress conditions, experiments involving high light intensity and elevated salinity were conducted to assess its ability to sustain C-PC production coupled to photosynthetic biogas upgrading.

2. Materials and methods

2.1. Nanoparticle solutions

The carbon-coated iron-based NPs investigated in this study were kindly provided by the Spanish companies CALPECH and SMALLOPS. These NPs were mainly produced from olive mill waste and iron salts. CALPECH NPs contained 8.7 wt% Fe, while SMALLOPS NPs contained 34.1 wt% Fe. The optical properties of each NPs were determined in terms of absorbance by preparing solutions with the corresponding tested concentration in modified Zarrouk media and measuring within the wavelength range of 440–800 nm. The complete physicochemical characterization of both NPs has been described in a previous study [15]. Before each batch experiment, a fresh stock solution containing 4 g·L^{-1} of the corresponding NP was prepared in *A. platensis* culture medium. The stock solution was sonicated for 1 h to prevent NP agglomeration and ensure homogeneous dispersion of the NPs throughout the cultivation system.

2.2. Microorganism and culture medium

Arthrospira platensis SAG 21.99 (commonly known as *Spirulina*) was obtained from the SAG culture collection of the University of Göttingen (Sammlung von Algenkulturen der Universität Göttingen). *A. platensis* cultures were maintained in Zarrouk medium composed of (per liter): 16.8 g $NaHCO_3$, 1 g NaCl, 0.04 g $CaCl_2$·2 H_2O, 2.5 g $NaNO_3$, 0.01 g $FeSO_4.7H_2O$, 0.08 g EDTA, 0.2 g $MgSO_4.7H_2O$, 0.5 g K_2HPO_4, and 1 mL of a micronutrient solution containing (per liter): $FeSO_4.7H_2O$ (0.07 g), $ZnSO_4.7H_2O$ (0.1 g), $MnCl_2.4H_2O$ (0.5 mg), H_3BO_3 (0.2 g), Co $(NO_3)_2.6H_2O$ (0.02 g), $Na_2MoO_4.2H_2O$ (0.02 g), $CuSO_4.5H_2O$ (0.5 mg) and EDTA.$2H_2O$ (1.02 g). The cultures were incubated at 25 ºC under illumination of 80 ± 10 µmol·m^{-2}·s^{-1}, provided by LED lights (Phillips, Spain) with a 12:12 h dark:light cycles.

Before each batch test, an inoculum of *A. platensis* was grown in a 2.1 L glass bottle with an effective liquid volume of 0.2 L of modified Zarrouk media, in which $NaHCO_3$ was reduced to 7 g·L^{-1}. To acclimate *A. platensis* to experimental conditions and shorten the lag phase, the headspace of the bottle was composed of synthetic biogas 70:30 (%, v/v) CH_4:CO_2 (Carburos metalicos, Spain). The inoculum was then incubated at a light intensity of 300 µmol·m^{-2}·s^{-1}, 25 ºC and 250 rpm, until the culture reached the exponential growth phase.

2.3. Experimental set-up

Batch experiments were conducted in 2.1 L glass bottles with a working volume of 0.2 L and a headspace of 1.9 L. Initially, the bottles were filled with modified Zarrouk medium (7 g·L^{-1} of $NaHCO_3$), sealed with butyl rubber septa and aluminium caps, and sterilized at 121 °C for 20 min. After cooling, the corresponding carbon-coated iron-based NPs were added to the sterile medium. The headspace was initially purged with helium for 10 min using inlet and outlet needles to remove atmospheric air and subsequently replaced with synthetic biogas (70:30, v/v, CH_4:CO_2) for an additional 10 min. Subsequently, the bottles were magnetically stirred at 250 rpm for 1 h to promote equilibrium between the gas and liquid phases. Finally, the bottles were inoculated with *A. platensis* to an initial optical density of 0.35 at 750 nm (OD_{750}). Cultures were incubated at 25 ± 2 °C under continuous illumination, provided by visible LED lights (Phillips, Spain) at a light intensity of 300 µmol·m^{-2}·s^{-1}, with constant agitation at 250 rpm to prevent sedimentation, enhance gas–liquid CO_2 transfer and maintain uniform exposure of cyanobacterial cells to the photic zone.

2.4. Experimental design

The influence of the NP type and concentration, light intensity and salinity on biogas upgrading and C-PC production was investigated through four distinct batch test series (A, B, C, D). Tests A and B were focused on evaluating the effects of CALPECH and SMALLOPS NPs, at different concentrations 50, 100, 150 mg·L^{-1}. In Test series C, the effect of the optimal NP type and concentration was evaluated at different light intensities (300 and 600 µmol·m^{-2}·s^{-1}). Finally, test series D examined the effect of optimal NP type and concentration addition on different salinity levels: 0.1, 0.3, 0.5 M NaCl. In test series A, B and C, a control without NPs was also run, whilst in test series D the control contained the optimal NP dose without salinity. All experimental trials were performed in biological duplicates. Independent replicate bottles were sampled to assess biological variability and ensure result reproducibility. Test durations were determined based on biomass growth and CO_2 uptake. In test series A, CALPECH NPs cultures remained active for up to 115 h, while SMALLOPS NPs cultures reached stationary phase after 103 h. Each trial concluded when CO_2 consumption and biomass growth stabilized.

2.5. Analytical procedures

A. platensis growth was monitored by measuring the OD_{750} of 2 mL using a spectrophotometer (UV-2550, Shimadzu Corporation, Japan), which was then converted to biomass concentration (g VSS·L^{-1}) using *ad-hoc* calibration curves. The pH was recorded using a pH meter (BASIC 20 +, Crison Instruments, Spain) equipped with a suitable electrode. The composition of biogas in the headspace of the bottle was analyzed using a gas chromatograph equipped with a thermal conductivity detector (GC–TCD, CP-3800, Varian, USA) following the methodology outlined

by Posadas et al. [19]. Dissolved inorganic carbon (IC), total organic carbon (TOC), total carbon (TC) and total nitrogen (TN) concentrations were determined using a Total Organic Carbon analyzer (TOC-VCSH, Shimadzu, Japan), fitted with a TNM-1 chemiluminescence module and an ASI-L autosampler (Shimadzu, Japan). Light intensity was measured using a quantum light meter (LI-250A LI-COR, Biosciences, Germany). Total Suspended Solids (TSS) and Volatile Suspended Solids (VSS) concentration were analyzed following standard methods [20]. The OD_{750}, pH and gas composition were measured twice a day, whereas IC, TOC, TC and TN concentration were determined at the beginning and end of each trial.

The specific growth rate (μ) was calculated using the natural logarithm of the biomass concentration during the exponential growth phase and the corresponding time according to Eq. (1):

$$\mu[d^{-1}] = \frac{\ln(X_2) - \ln(X_1)}{t_2 - t_1} \quad (1)$$

where μ is the specific growth rate (d^{-1}), X_1 and X_2 are the biomass concentrations (g TSS·L^{-1}) at times t_1 and t_2 (d), respectively.

The biomass productivity (P_x) of *A. platensis* was calculated using the biomass concentration during the exponential growth phase and the corresponding time, as shown in Eq. (2):

$$P_X \quad [gTSS \bullet L^{-1} \bullet d^{-1}] = \frac{X_2 - X_1}{t_2 - t_1} \quad (2)$$

where P_x is the biomass productivity (gTSS·L^{-1}·d^{-1}) [21].

C-PC concentration was determined by taking 2 mL samples, followed by centrifugation (11,000 × g, 5 min). The supernatant was carefully removed and 1 mL of 0.1 M phosphate buffer (pH 7.0) was added to the pellet. Then, the C-PC was extracted through 3 freeze-thaw cycles followed by centrifugation (11,000 × g, 5 min). The absorbance of the resulting supernatant was measured at 620 nm and 650 nm, and the C-PC concentrations were calculated based on the Eq. (3) [18,22]:

$$C_{C-PC} \quad [mg \bullet mL^{-1}] = \frac{A_{620} - 0.474 * A_{650}}{5.34} \quad (3)$$

where $C_{C\text{-}PC}$ is phycocyanin concentration in the extract (mg·mL^{-1}), while A_x indicates the absorbance of the final extract at wavelength x (nm); The resulting C-PC values were expressed as milligrams of phycocyanin per gram of dry biomass (mg·g^{-1}).

2.6. Statistical analysis

All treatments were performed in duplicate. Results were expressed as mean ± standard deviation of biological duplicates. Statistical differences among groups were evaluated using one-way analysis of variance (ANOVA), followed by Tukey's test. A p-value < 0.05 was considered statistically significant. Analyses were conducted using IBM SPSS Statistics for Windows, Version 27.0 (IBM Corp., Armonk, NY, USA). A Principal Component Analysis (PCA) was performed using the Orange Data Mining v.3.38.1 software for investigating the effects of the two carbon-coated iron-based NPs on *A. platensis* growth (biomass concentration, O_2 production), biogas upgrading (CO_2 consumption) and C-PC accumulation in *A. platensis* [23].

3. Results and discussion

3.1. Effect of nanoparticles on CO_2 assimilation, growth and phycocyanin content of A. platensis

The addition of CALPECH NPs at varying concentrations enhanced the metabolic activity of *A. platensis*, primarily by accelerating growth and increasing biomass concentration under batch cultivation. As illustrated in Fig. 1a, the presence of CALPECH NPs increased CO_2 uptake compared to the control over the 115-hour cultivation period, with CO_2 concentration reaching 32 % at 100 mg·L^{-1}, followed by a 29 % at 50 mg·L^{-1} and 25 % in the control assays. This enhanced metabolic activity was further demonstrated by significant increases in specific growth rate and biomass productivity, with the highest values observed at a CALPECH NP concentration of 100 mg·L^{-1} (μ = 0.69 d^{-1}, P_x = 0.97 g TSS·L^{-1}·d^{-1}), surpassing the control (μ = 0.57 d^{-1}, P_x = 0.60 g TSS·L^{-1}·d^{-1}). This growth enhancement was also reflected in the significant reduction in the final IC levels, which decreased from 543 mg·L^{-1} in the control to 355 mg·L^{-1} at 100 mg·L^{-1} of CALPECH NPs. This intense IC consumption can be attributed to an increased photosynthetic activity induced by CALPECH NPs addition, which mediated a more efficient carbon and nitrogen assimilation as shown in Table 1 [24]. Similarly, the growth of *A. platensis* was also improved, with the highest biomass concentration reaching 3.5 g VSS·L^{-1} at 100 mg·L^{-1}, in contrast to the 2.3 g VSS·L^{-1} observed in the control (Fig. 1e). Similar biomass concentrations were reported by Vargas-Estrada et al. [24] in a high rate algal pond (HRAP) after the addition of 70 mg·L^{-1} of carbon coated zero-valent iron NPs. Comparably, Hoyos et al. [14] observed an increased biomass concentration up to 3.1 g VSS·L^{-1} induced by the addition of 140 mg·L^{-1} of the same NPs in a HRAP system. However, when CALPECH NPs concentration was increased to 150 mg·L^{-1}, a reduction in CO_2 consumption and O_2 production was observed.

At this point, it is important to stress that the UV–VIS spectra of the CALPECH NPs solutions (Fig. 2) showed increased absorbance with higher NP concentrations, substantially reducing light penetration into the cultures. The stimulatory effect was evident after 24 h of cultivation, with NP-supplemented cultures entering the exponential growth phase approximately 24-h earlier than the controls. Moreover, the UV–VIS spectra of CALPECH NPs exhibited characteristic $\pi \rightarrow \pi^*$ transitions, with higher peaks observed in the range of 240–290 nm. Although the position of $\pi \rightarrow \pi^*$ transitions is intimately related to the structure of the material [25], phenolic compounds, such as graphene, humic acids, flavonoids (A ring), and other aromatics, typically absorb within this range. These chemical compounds, particularly humic acids, have been reported to exert hormetic effects in microalgae, plants and bacteria due to their capacity to transfer electrons, chelate metals and activate antioxidant enzymes [26]. Accordingly, increasing the NP concentration resulted in a higher abundance of phenolic compounds, as reflected in Fig. 2, likely leading to an increased electron flux that boosted the metabolic activity of *A. platensis* cultures. Interestingly, when 150 mg·L^{-1} CALPECH NPs were added, the hormetic effects of the NPs remained evident. Indeed, cultures supplemented with 150 mg·L^{-1} CALPECH NPs presented the same accelerated growth pattern as those supplemented with 50 and 100 mg·L^{-1} CALPECH NPs, particularly at the beginning of the exponential phase, however, their final performance was lower compared to cultures receiving lower NPs doses. Thereby, it can be hypothesized that the reduced beneficial effects of the NPs at the highest concentration tested were likely due to the hormetic effects of phenolic compounds. In this context, Toropkina et al. [27] observed that adding 0.001 – 0.003 % humic acids enhanced the photosynthetic activity and biomass production of *Chlorella vulgaris* (*C. vulgaris*), whereas concentrations above 0.003 % inhibited growth. Similarly, the growth of *Scenedesmus capricornus* (*S. capricornus*) was promoted by 17 % when 0.5 mgC L^{-1} of humic acids were added to the cultures, whilst concentrations above 2 mg L^{-1} inhibited *S. capricornus* growth [28]. Nonetheless, *A. platensis* cultures supplemented with 150 mg·L^{-1} CALPECH NPs still outperformed control cultures (0 mg·L^{-1} NPs).

CALPECH NPs positively influenced C-PC content in *A. platensis* cultures. Cultures supplemented with 100 mg·L^{-1} CALPECH NPs achieved a C-PC concentration of 180 mg·g^{-1}, representing an approximately 59 % increase compared to the control (113 mg·g^{-1}). This enhancement in C-PC content was closely followed by cultures supplemented with 50 mg·L^{-1}, which accumulated a C-PC content of 169 mg·g^{-1}, and by those supplemented with 150 mg·L^{-1}, which

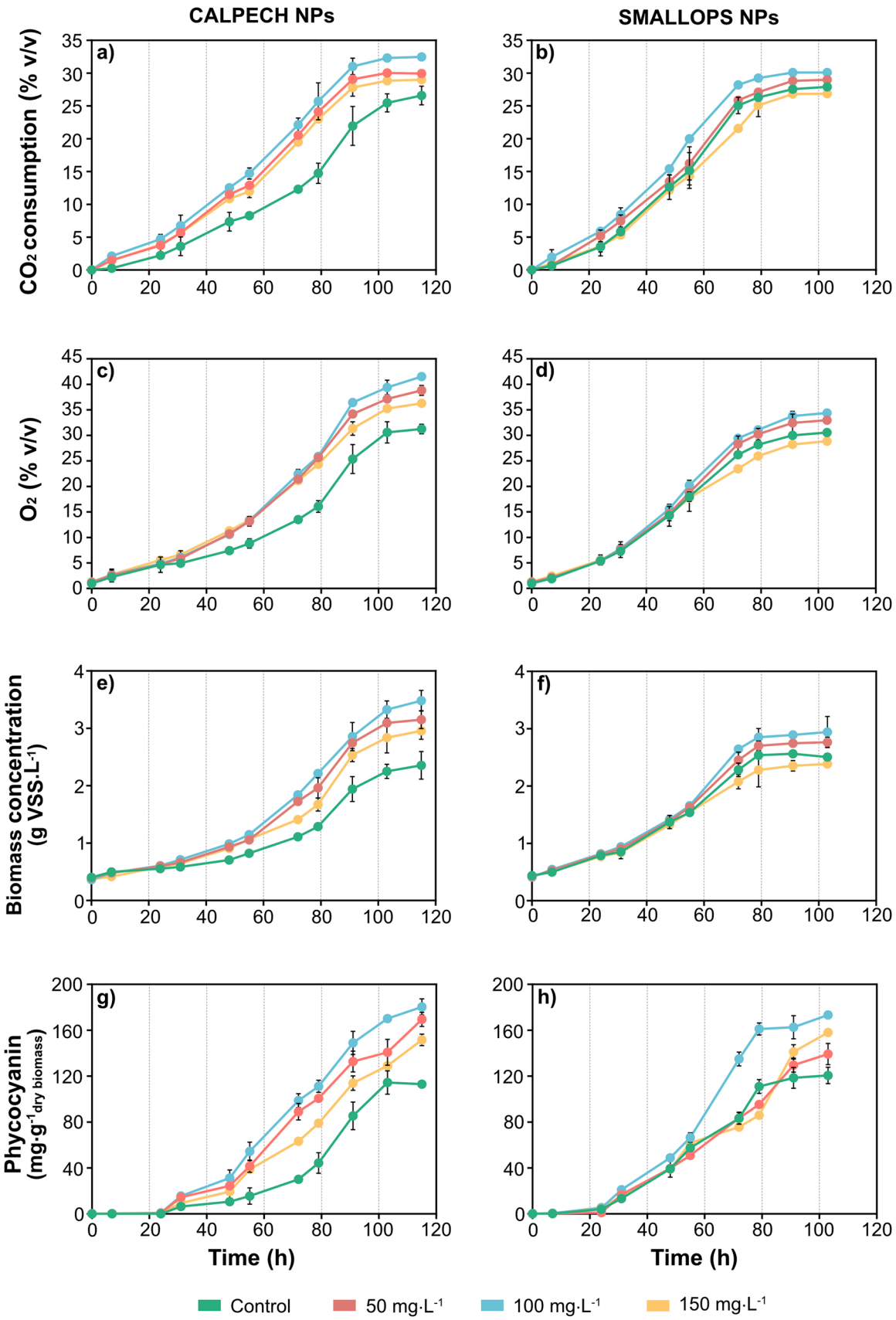

Fig. 1. Time course of key photosynthetic and growth parameters during *A. platensis* cultivation with CALPECH and SMALLOPS NPs. a) CO_2 consumption (% v/v), b) O_2 production (% v/v), c) biomass concentration (g VSS·L^{-1}) and d) phycocyanin content (mg·g^{-1} biomass) with CALPECH NPs; and a) CO_2 consumption (% v/v), b) O_2 production (% v/v), c) biomass concentration (g VSS·L^{-1}) and d) phycocyanin content (mg·g^{-1} biomass) with SMALLOPS NPs at different concentrations: control (green), 50 mg·L^{-1} (red), 100 mg·L^{-1} (blue), 150 mg·L^{-1} (yellow). Data are presented as mean ± standard deviation (n = 2). VSS: Volatile Suspended Solids.

Table 1
Biomass productivity (P_x), specific growth rate (μ) and initial and final inorganic carbon (IC), total organic carbon (TOC), total nitrogen (TN) concentration ($mg{\cdot}L^{-1}$) and pH values in *A. platensis* batch cultures with addition of CALPECH NPs at the concentrations of 50, 100, and 150 $mg{\cdot}L^{-1}$.

CALPECH NPs				
Parameter	**Control**	**50 $mg{\cdot}L^{-1}$**	**100 $mg{\cdot}L^{-1}$**	**150 $mg{\cdot}L^{-1}$**
μ (d^{-1})	0.57 ± 0.04	0.67 ± 0.01	0.69 ± 0.00	0.64 ± 0.00
P_x (g TSS·L^{-1}·d^{-1})	0.60 ± 0.08	0.91 ± 0.02	0.97 ± 0.07	0.84 ± 0.03
$IC_{initial}$ ($mg{\cdot}L^{-1}$)	1133.09 ± 1.09	1153.88 ± 34.02	1090.26 ± 27.00	1139.99 ± 13.20
IC_{final} ($mg{\cdot}L^{-1}$)	542.55 ± 77.00	416.58 ± 51.13	355.00 ± 22.11	377.63 ± 41.02
$TOC_{initial}$ ($mg{\cdot}L^{-1}$)	44.00 ± 35.00	41.91 ± 2.17	41.37 ± 25.13	42.77 ± 5.22
TOC_{final} ($mg{\cdot}L^{-1}$)	270.77 ± 17.03	623.58 ± 10.08	712.81 ± 2.74	492.60 ± 39.00
$TN_{initial}$ ($mg{\cdot}L^{-1}$)	436.97 ± 2.44	426.39 ± 5.12	423.47 ± 5.55	424.08 ± 2.70
TN_{final} ($mg{\cdot}L^{-1}$)	285.05 ± 0.29	235.55 ± 1.08	199.82 ± 1.90	260.25 ± 5.87
$pH_{initial}$	7.61 ± 0.05	7.59 ± 0.08	7.57 ± 0.05	7.55 ± 0.04
pH_{final}	9.00 ± 0.01	9.86 ± 0.01	10.05 ± 0.03	9.49 ± 0.18

*TSS: Total Suspended Solids

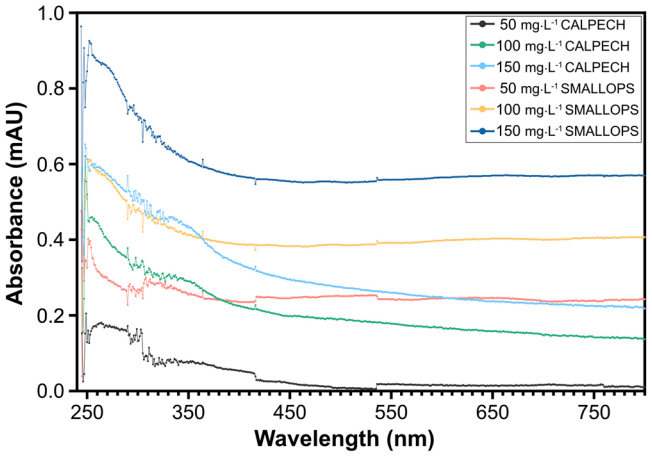

Fig. 2. UV–VIS spectra of the CALPECH and SMALLOPS NPs solutions at different concentrations. Spectra illustrate absorbance values across wavelengths for NPs at 50, 100, and 150 $mg{\cdot}L^{-1}$.

reached 152 $mg{\cdot}g^{-1}$ (Fig. 1g). Interestingly, the addition of the NPs triggered the accumulation of C-PC at the beginning of the exponential phase, suggesting that the reduced light availability caused by NPs positively affected C-PC synthesis. In this context, previous studies have demonstrated that *A. platensis* cultures produced higher C-PC concentrations under low light intensity. For instance, the C-PC content of *A. platensis* cultures decreased from 74 to 56 $mg{\cdot}g^{-1}$ when the light intensity was increased from 100 to 203 $\mu mol{\cdot}m^{-2}{\cdot}s^{-1}$ [29]. Moreover, according to Chaiklahan et al. [30] C-CP content decreased from approximately 200 $mg{\cdot}g^{-1}$ at 100 $\mu mol{\cdot}m^{-2}{\cdot}s^{-1}$ to 25 $mg{\cdot}g^{-1}$ at 500 $\mu mol{\cdot}m^{-2}{\cdot}s^{-1}$. However, at a NPs concentration of 150 $mg{\cdot}L^{-1}$, a reduction in C-PC levels was observed, likely due to stress conditions that limited C-PC synthesis [31]. Indeed, a high concentration of phenolic-based compounds, including humic acids, can induce oxidative stress in microalgae species such as *Chlorella* sp. or *Coelastrella* sp. Thus, the elevated NPs concentration could have triggered oxidative stress in *A. platensis* cultures, thereby reducing the C-PC content compared to the cultures supplemented with 50 and 100 $mg{\cdot}L^{-1}$ NPs [32,33]. Moreover, the increased NPs concentration could have induced an electron flux beyond the tolerance of *A. platensis*, thereby reducing C-PC levels as a protective response to prevent excessive electron formation [34].

On the other hand, the addition of SMALLOPS NPs at 100 $mg{\cdot}L^{-1}$ resulted in a marked increase in CO_2 consumption during the cultivation period (Fig. 1b), with a final CO_2 content of 30 ± 0.01 % compared to the 27 ± 0.15 % in the control. The presence of 100 $mg{\cdot}L^{-1}$ SMALLOPS NPs to the culture broth enhanced the metabolism of *A. platensis* during batch biogas upgrading, as evidenced by the higher specific growth rate (μ = 0.78 d^{-1}) and biomass productivity (P_x = 0.90 g TSS·L^{-1}·d^{-1}) compared to the control (μ = 0.69 d^{-1}, P_x = 0.73 g TSS·L^{-1}·d^{-1}). This improvement coincided with a measurable reduction in the final IC concentration, which decreased from 863 $mg{\cdot}L^{-1}$ in the control to 810 $mg{\cdot}L^{-1}$ in the assay supplemented with 100 mg NP·L^{-1}. This decrease suggests an improved assimilation of CO_2 facilitated by the NPs. The production of O_2 was also slightly higher at 100 $mg{\cdot}L^{-1}$, reaching a final concentration of 34 % compared to the control (30 %), although this difference was not statistically significant (Fig. 1d). At this point it is important to highlight that SMALLOPs NPs seem to contain traces of phenolic compounds (Fig. 2), which can be inhibitory for microalgae. In fact, the initial TOC concentration increased with increasing SMALLOPS NPs concentration (Table 2). Moreover, SMALLOPS NPs exhibited higher absorbance within the wavelength range corresponding to Chlorophyll a, and C-PC light absorption, potentially reducing the growth performance of supplemented cultures. Nevertheless, a modest increase in biomass concentration, peaking at 2.9 g VSS·L^{-1} in the assays supplemented with 100 $mg{\cdot}L^{-1}$, was recorded compared to a slightly lower value of 2.5 g VSS·L^{-1} in the control (Fig. 1f). The analysis of TOC, TC, TN concentrations and pH values (Table 2) at the end of the cultivation further supported the finding that 100 $mg{\cdot}L^{-1}$ SMALLOPS NPs promoted *A. platensis* growth. However, at 150 $mg{\cdot}L^{-1}$, both *A. platensis* growth and biogas upgrading efficiency declined compared to the control. This reduced *A. platensis* performance could be attributed to the hormetic effects of phenolic compounds present in the NPs, which surpassed *A. platensis* tolerance. Phenolic compounds (including humic acids) are well-known stimulants of microalgae and plants when applied at low concentrations (< 20 $mg{\cdot}L^{-1}$), but higher often produce detrimental effects due to the induction of oxidative stress. In such conditions, O_2 acts as an electron acceptor, generating reactive oxygen species (ROS), including superoxide free radicals [32].

Table 2
Biomass productivity (P_x), specific growth rate (μ) and initial and final inorganic carbon (IC), total organic carbon (TOC), total nitrogen (TN) concentration ($mg{\cdot}L^{-1}$) and pH values in *A. platensis* batch cultures with addition of SMALLOPS NPs at the concentrations of 50, 100, and 150 $mg{\cdot}L^{-1}$.

SMALLOPS NPs				
Parameter	**Control**	**50 $mg{\cdot}L^{-1}$**	**100 $mg{\cdot}L^{-1}$**	**150 $mg{\cdot}L^{-1}$**
μ (d^{-1})	0.69 ± 0.00	0.71 ± 0.01	0.78 ± 0.00	0.68 ± 0.03
P_x (g TSS·L^{-1}·d^{-1})	0.73 ± 0.03	0.80 ± 0.04	0.90 ± 0.01	0.69 ± 0.03
$IC_{initial}$ ($mg{\cdot}L^{-1}$)	1183.68 ± 20.00	1020.63 ± 1.34	1052.33 ± 39.02	1074.31 ± 37.11
IC_{final} ($mg{\cdot}L^{-1}$)	863.27 ± 94.03	879.08 ± 78.00	810 ± 32.08	1104.59 ± 8.06
$TOC_{initial}$ ($mg{\cdot}L^{-1}$)	49.76 ± 7.70	69.13 ± 3.94	78.90 ± 8.45	65.10 ± 3.41
TOC_{final} ($mg{\cdot}L^{-1}$)	65.56 ± 16.00	130.50 ± 7.12	158.80 ± 54.85	95.87 ± 14.47
$TN_{initial}$ ($mg{\cdot}L^{-1}$)	348.54 ± 21.16	350.47 ± 15.20	364.90 ± 1.29	355.65 ± 3.73
TN_{final} ($mg{\cdot}L^{-1}$)	270.50 ± 7.71	210.50 ± 12.16	160.88 ± 10.10	295.27 ± 12.03
$pH_{initial}$	7.64 ± 0.02	7.57 ± 0.10	7.67 ± 0.05	7.75 ± 0.02
pH_{final}	9.11 ± 0.04	9.46 ± 0.07	9.52 ± 0.26	9.21 ± 1.05

*TSS: Total Suspended Solids

Finally, the C-PC content reached a maximum of 173 mg·g^{-1} at 100 mg NP·L^{-1}, followed by 158 mg·g^{-1} and 139 mg·g^{-1} at 150 and 50 mgNP·L^{-1}, respectively, compared to the lowest value of 120 mg·g^{-1} observed in the control assay (Fig. 1h). Interestingly, the addition of 100 mg·L^{-1} SMALLOPS NPs increased the C-PC content from the beginning of the exponential phase, whereas cultures supplemented with 50 and 150 mg NP·L^{-1} exhibited patterns similar to the control. Despite the higher iron content of the SMALLOPS NPs may have induced an oxidative stress on *A. platensis* cultures, no significant reduction in C-PC content was observed compared to CALPECH NPs ($p > 0.05$). Similar findings have been reported by Ismaiel et al. [35], who found that increasing iron concentrations did not enhance C-PC content of *A. platensis*, despite the essential role of iron in photosynthetic pigment synthesis. Thus, the increased C-PC content in *A. platensis* cultures supplemented with SMALLOPS NPs was likely due to the stimulating effect of phenolic compounds present in the NPs rather than to the iron content.

A PCA analysis was performed to evaluate the effect of carbon-coated iron-based NPs at different concentrations on four measured responses: final biomass concentration, biogas upgrading (CO_2 consumption and O_2 production) and C-PC content. The PCA plot (Fig. 3) of the two iron-based NPs showed that the first two principal components accounted for 59.8 % of the total variance in the dataset, with PC1 and PC2 explaining 35.3 % and 24.5 %, respectively. This indicates that these two components captured a significant part of the overall variability, providing a meaningful overview of the NPs effects on the measured responses. The PCA plot revealed that the analyzed samples were grouped into two distinct clusters based on their similarities. In particular, CALPECH and SMALLOPS NPs did not overlap, suggesting that they exerted different effects on the responses. This distinction confirms that each NP exhibits a unique profile across the four measured responses. Within the CALPECH NP group, all concentrations were clearly distributed along the PC1 axis. This was particularly evident between the control (0 mg·L^{-1}) and the 100 mgNP·L^{-1} treatment, which are placed far apart on the plot, indicating that their effects on the responses were different and significant. In contrast, in the SMALLOPS NP group, the different concentrations were closely together with limited dispersion, suggesting that the use of various concentration did not have a strong impact on the responses. Overall, the PCA plot suggests that the concentrations of CALPECH NP produced more distinct effect on regulating the responses of *A. platensis* in batch cultures.

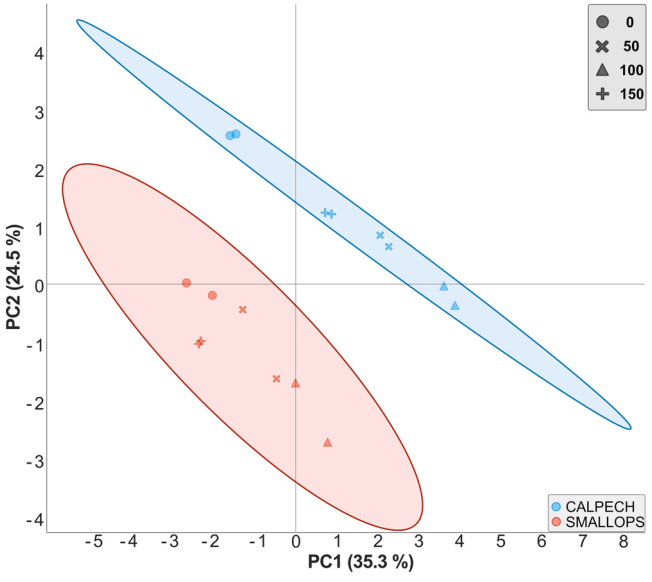

Fig. 3. Principal Component Analysis (PCA) plot illustrating the effect of CALPECH (blue) and SMALLOPS (red) NPs at different concentrations. Marker shapes correspond to concentrations of 0 (circle), 50 (cross), 100 (triangle), and 150 mg·L^{-1} (plus) on biomass concentration, biogas upgrading (CO_2 consumption and O_2 production) and phycocyanin production. The axes (PC1, PC2) represent the principal components explaining the largest variance among the samples.

These findings revealed that the supplementation of iron-based NPs at nearly all tested concentrations significantly enhanced *A. platensis* growth and CO_2 consumption in batch cultures. This improvement can be attributed to the presence of phenolic compounds, the attenuated light availability and the iron content in the NPs. Iron is an essential trace element that support cyanobacterial growth and photosynthesis by acting as a redox catalyst in electron transport reactions [36]. Although the iron content of the NPs varied significantly, *A. platensis* did not experience notable growth inhibition following the addition of the two NPs, particularly the SMALLOPS NPs, as this species is known to tolerate relatively high iron concentrations [37]. Both CALPECH and SMALLOPS NPs are coated with carbon, on which their positive biostimulant nature relies, as low concentrations of phenolic compounds have been shown to enhance microalgal metabolism [38]. Certainly, the specific phenolic compounds of each NP are intimately related to the nature of their precursors, with SMALLOPS NPs exhibiting a higher phenolic compound concentration, which significantly influenced *A. platensis* performance. Hence, CALPECH NPs demonstrated higher growth stimulation and greater efficiency in the biogas upgrading process than SMALLOPS NPs under the same experimental conditions. These differences are primarily attributed to variations in their physicochemical properties, morphology and iron content. Among all the above tested cultivations with the two carbon-coated iron-based NPs under different concentrations, CALPECH NPs at 100 mg·L^{-1} provided the greatest enhancement in *A. platensis* growth, CO_2 consumption and C-PC content, and were therefore selected for subsequent batch experiments.

3.2. *Effect of nanoparticle addition and light intensity on CO_2 assimilation, growth and phycocyanin content of A. platensis cultures*

The beneficial effects of CALPECH NPs at the optimal concentration of 100 mg·L^{-1} on *A. platensis* growth and C-PC synthesis were evaluated under different light intensities. The addition of 100 mg·L^{-1} of CALPECH NPs under light intensities of 300 and 600 μmol·m^{-2}·s^{-1} significantly enhanced CO_2 consumption ($p < 0.05$), reaching a CO_2 concentration of 33 % at both light intensities, compared to 29 % and 25 % at 300 and 600 μmol·m^{-2}·s^{-1} without NPs, respectively (Fig. 4a). O_2 production in assays with NPs followed a similar trend, showing a slight increase to 44 % at 600 μmol·m^{-2}·s^{-1} compared to 41 % at 300 μmol·m^{-2}·s^{-1}. In contrast, O_2 production in the absence of NPs was higher at 300 μmol·m^{-2}·s^{-1} (31 %) than at 600 μmol·m^{-2}·s^{-1} (18 %), corresponding to a 42 % reduction in photosynthetic efficiency (Fig. 4b). This decline was mainly attributed to the formation of ROS, which are typically produced when light intensity exceeds the capacity of microalgae to absorb light [39]. Hence, the protective action of the NPs can likely be ascribed to antioxidant compounds present on their surface, that acted as light scavengers and prevented oxidative damage in cultures exposed to a high light intensity. Indeed, CALPECH NPs enhanced growth at both tested light intensities, with the most pronounced effect observed at 600 μmol·m^{-2}·s^{-1}. Under this condition, the specific growth rate increased from 0.55 to 0.67 d^{-1}, and P_X rose from 0.61 to 1.06 g TSS·L^{-1}·d^{-1}. Additionally, IC levels decreased by 49 %, confirming the stimulation of metabolic activity in the presence of NPs (Table S1). The evolution of biomass concentration in the presence of NPs mirrored these patterns, with significant increases up to 3.4 g VSS·L^{-1} and 3.6 g VSS·L^{-1} at 300 and 600 μmol·m^{-2}·s^{-1}, respectively, compared to 1.9 g VSS·L^{-1} and 1.6 g VSS·L^{-1} in the absence of NPs ($p < 0.05$) (Fig. 4c). The TOC, TC, TN concentrations and pH values (Table S1) further supported that the addition of 100 mg·L^{-1} CALPECH NPs prevented photoinhibition of *A. platensis* at the highest light intensity. Although biomass concentrations were consistently higher at 600 μmol·m^{-2}·s^{-1} than at 300 μmol·m^{-2}·s^{-1} in the presence of NPs, the

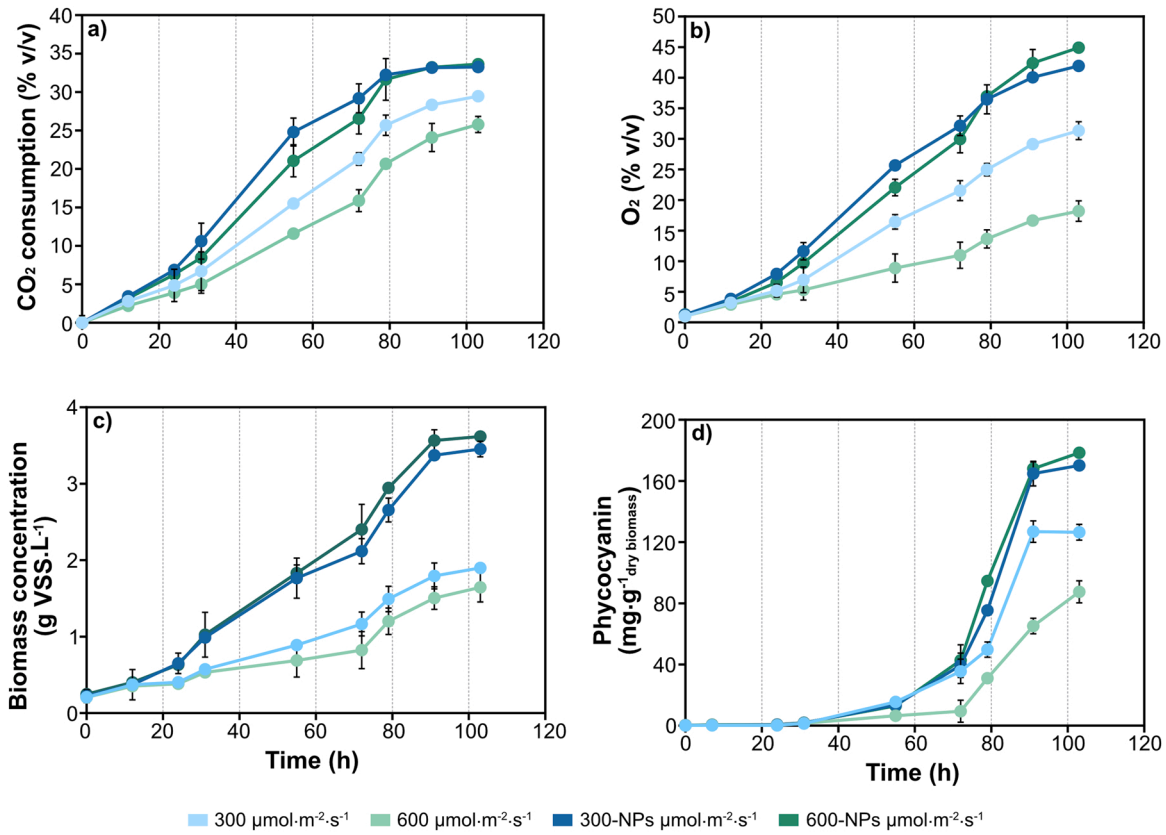

Fig. 4. Time course of photosynthetic and growth parameters during A. platensis cultivation under different light intensities with and without CALPECH NPs supplementation. a) CO_2 consumption (% v/v), b) O_2 production (% v/v), c) biomass concentration (g VSS·L^{-1}) and d) phycocyanin content (mg·g^{-1} biomass) under 300 µmol·m^{-2}·s^{-1} (light blue), 300 µmol·m^{-2}·s^{-1} + NPs (blue), 600 µmol·m^{-2}·s^{-1} (green), 600 µmol·m^{-2}·s^{-1} + NPs (dark green). Data are presented as mean ± standard deviation (n = 2). VSS: Volatile Suspended Solids.

difference between the two light intensities was not statistically significant. This suggests that CALLPECH NPs supplementation mitigated the effects of increased light and maintained stable growth performance under both conditions.

C-PC synthesis was also enhanced by the addition of NPs, reaching a maximum of 178 mg·g^{-1} at 600 µmol·m^{-2}·s^{-1} with NPs, followed by 170 mg·g^{-1} at 300 µmol·m^{-2}·s^{-1}. In contrast, although biomass concentrations of *A. platensis* cultures in the absence of NPs supplementation were similar at both light intensities, the C-PC content was significantly reduced to 87 mg·g^{-1} at 600 µmol·m^{-2}·s^{-1} (Fig. 4d). These findings confirm that NPs acted as protective agents against the oxidative damage mediated by the increased light intensity. Numerous studies have shown that NPs tend to accumulate on the surface of photosynthetic microorganisms, forming aggregates that may reduce light penetration to the underlying algal cells. This observation aligns with the fact that the typical cell wall pore diameter of microalgae ranges from 5 to 20 nm, which is considerably smaller than many NPs used in cultivation systems. Consequently, surface accumulation likely creates a physical barrier or shading effect that limits excessive light and nutrient penetration, thereby protecting cells from photodamage. Although direct microscopic evidence of NP internalization within *Arthrospira* filaments is limited, SEM and EDX analyses in similar microalgal systems consistently indicate that extracellular localization is the predominant mechanism of NP interaction [40–42].

While light is essential for promoting photosynthesis, excessive exposure in the absence of NPs can impair this process due to photo-oxidative stress, leading to reduced photosynthetic efficiency, a phenomenon known as photoinhibition [43]. Yang et al. [44] demonstrated that graphene oxide quantum dots improved photosynthetic efficiency and CO_2 fixation in *Chlorella pyrenoidosa* cultivation by mitigating UV stress. Similarly, iron NPs have been shown to enhance photosynthesis and carbon fixation by scavenging ROS and improving iron bioavailability, which is essential for electron transport and enzymatic processes [45–48]. Moreover, Vargas-Estrada and co-workers demonstrated that the addition of carbon-coated zero-valent iron NPs scavenged UV-light stress in a mixed microalgae-bacteria consortium, and in *Chlorella sorokiniana* cultures devoted to biogas upgrading [15,49]. Some NPs also exhibit light-harvesting properties, compensating for inefficient light utilization commonly observed in dense algal cultures [48]. In contrast, in the absence of NPs, a high light intensity negatively affected C-PC production, aligning with earlier studies indicating that lower light intensities favor pigment accumulation in *A. platensis*. Schipper et al. [50] reported that low light intensities (~ 80 µmol·m^{-2}·s^{-1}) tend to promote higher C-PC content in microalgal species, including *A. platensis*, while higher intensities (300–1800 µmol·m^{-2}·s^{-1}) reduce pigment levels by 53 % and 79 %. Similarly, Xie et al. [51] observed an initial increase in pigment productivity up to 40 mg·L^{-1}·d^{-1} when irradiation increased from 75 to 300 µmol·m^{-2}·s^{-1}, followed by a decline to approximately 1 mg·L^{-1}·d^{-1} at 450 µmol·m^{-2}·s^{-1}, indicating that photoinhibition may occur beyond a certain light threshold. This reduction could be due to the fact that cells achieved a sufficient light absorption, thereby reducing the need for C-PC as a light-harvesting pigment. Certainly, cultures exposed to 600 µmol·m^{-2}·s^{-1} without the addition of NPs exhibited delayed C-PC synthesis, which became evident only during the exponential phase, indicating that self-shading within *A. platensis* may have triggered C-PC formation. Overall, the above findings underscore the photoinhibition mitigation potential of NPs supplementation to *A. platensis* cultures while simultaneously promoting growth, CO_2 capture, C-PC production, and resistance to oxidative stress.

3.3. Effect of salinity and NPs supplementation on CO_2 assimiliation, growth and C-PC content of A. platensis cultures

Salinity is another environmental factor that influences the growth, productivity and photosynthetic performance of *A. platensis* [52,53]. Moderate salinity levels can stimulate pigment biosynthesis by upregulating related gene expression, whereas excessive salinity induces osmotic and oxidative stress, disrupting cellular metabolism and ultimately inhibiting photosynthesis [54,55]. Recent studies have demonstrated that NPs supplementation can enhance algal growth and improve salinity tolerance by regulating hormone levels, antioxidant activity, ion balance, and the expression of stress-related genes [56,57].

The impact of different salinity levels on *A. platensis* growth and biogas upgrading was evaluated in the presence of 100 mg·L^{-1} of CALPECH NPs. This approach provides valuable insight into strategies for improving microalgal growth and pigment synthesis by assessing whether CALPECH NPs enhance *A. platensis* tolerance to saline conditions. The metabolic impact of NPs supplementation on *A. platensis* was comprehensively assessed by monitoring CO_2 consumption, O_2 production, biomass concentration, and phycocyanin content, which represent robust physiological and biochemical indicators commonly used in microalgae process studies [58–60]. As shown in Fig. 5a, culture exposure to 0.1 M NaCl resulted in the highest CO_2 consumption (35 %), closely followed by the control (34 %), while cultures supplemented with 0.3 M and 0.5 M NaCl showed lower consumption levels of 30 % and 28 %, respectively. Although the slight increase in NaCl concentration up to 0.1 M did not result in a significant difference in CO_2 uptake compared to the control, further increases in salinity reduced CO_2 capture efficiency. O_2 production exhibited a similar trend, with a slight increase to 42 % at 0.1 M compared to 40 % in the control (Fig. 5b). A maximum biomass concentration of 3.0 g VSS·L^{-1} was observed at 0.1 M salinity, decreasing to 2.15 g VSS·L^{-1} and 1.98 g VSS·L^{-1} at 0.3 M and 0.5 M, respectively (Fig. 5c). These results were further supported by biomass productivity, specific growth rate, final IC, TOC, TN concentrations and pH values at the end of the trials (Table S2). Hence, the addition of NPs mitigated the inhibitory effects of salinity in cultures exposed to 0.1 M NaCl, even though salinity stress typically increases the energy demand required to maintain turgor pressure, thereby limiting biomass growth [35].

The production of C-PC exhibited a trend similar to that of biomass concentration. The final C-PC concentration reached 179 mg·g^{-1} in the control and 193 mg·g^{-1} at 0.1 M NaCl. However, the increase in NaCl to 0.3 M and 0.5 M induced a decrease of C-PC content by 16.5 % and 48.5 %, respectively (Fig. 5d). Despite the observed decrease in C-PC content with increasing salinity, the results obtained herein were significantly higher than those obtained by Ismaiel et al. [35], who reported C-PC contents ranging between 60 and 130 mg g^{-1} in *A. platensis* cultures exposed to 0.04–0.34 M NaCl. This confirms the beneficial role of NPs supplementation in enhancing C-PC synthesis and *A. platensis* metabolism.

Among all the tested salinity levels, 0.1 M NaCl consistently supported the highest growth, CO_2 consumption, O_2 production, and C-PC content, closely followed by the control. In contrast, salinities above 0.1 M negatively impacted *A. platensis* cultures. These results are in agreement with Sujatha and Nagarajan [61], who reported that *A. platensis* growth and C-PC production increased approximately to 110 mg g^{-1} at 0.1 M and 0.2 M concentrations, and decreasing approximately to 80 and 60 mg g^{-1} at 0.3 M and 0.4 M. Previous studies have also shown that deviations from the optimal salinity can disrupt ionic balance and photosynthetic processes, leading to morphological and physiological changes that reduce *A. platensis* productivity [62,63]. High salt concentrations impair metabolism, inhibit growth and photosynthesis, and induce oxidative stress through the accumulation of ROS, which damage cellular components and alter metabolic pathways

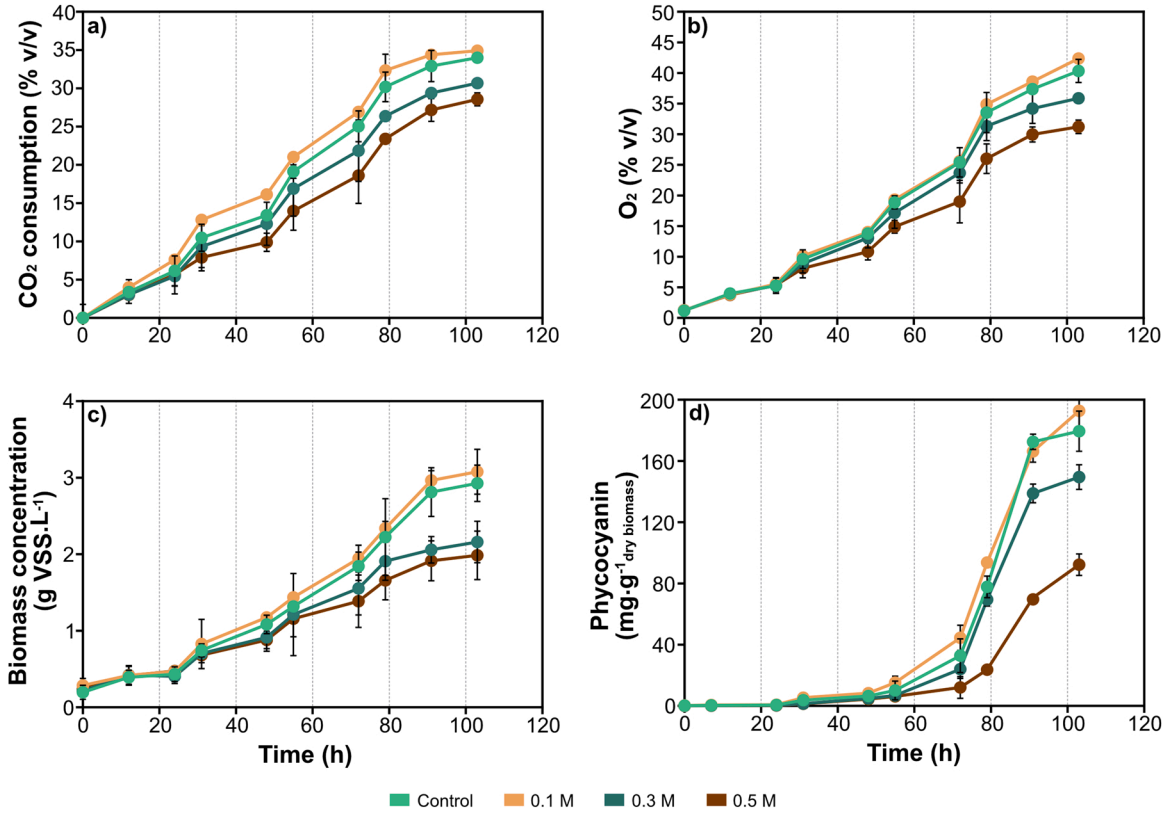

Fig. 5. Time course of photosynthetic and growth parameters during *A. platensis* cultivation under different salinities with 100 mg·L^{-1} of CALPECH NPs. a) CO_2 consumption (% v/v), b) O_2 production (% v/v), c) biomass concentration (g VSS·L^{-1}) and d) phycocyanin content (mg·g^{-1} biomass) at control (green), 0.1 M NaCl (light brown), 0.3 M NaCl (dark green), 0.5 M NaCl (dark brown). Data are presented as mean ± standard deviation (n = 2). VSS: Volatile Suspended Solids.

[64–66]. Specifically, ROS accumulation damages photosystems, reducing oxygen release [67]. Additional ROS, malondialdehyde (MDA), and antioxidant enzyme analyses are needed for a deeper understanding of oxidative stress mechanisms. As described in Section 3.2, the addition of NPs improved CO_2 consumption and photosynthetic activity in *A. platensis* cultures by scavenging ROS, boosting antioxidant defenses and regulating stress response pathways, particularly at low salinities (0.1 M NaCl) [68]. However, at salinities above 0.1 M NaCl, biomass productivity decreased, leading to a reduced CO_2 biofixation by *A. platensis* cultures even with NPs supplementation [69]. Nonetheless, *A. platensis* demonstrated robust growth across a range of salinities, with optimal growth occurring at lower salinity levels.

Beyond the physiological responses observed under NPs supplementation, *A. platensis* biomass cultivated in Zarrouk medium enriched with carbon-coated iron-based NPs holds promising potential for downstream applications. The harvested biomass can be further valorized for the production of bioactive compounds with uses in pharmaceutical, nutraceutical, environmental, food, and agricultural sectors. NPs can be efficiently separated from the biomass using conventional methods such as centrifugation, gravity settling, filtration, or dissolved air flotation. Magnetic separation, in particular, offers a highly effective and sustainable approach due to the intrinsic magnetic properties of iron-based NPs [70,71]. Furthermore, the NPs can be efficiently recovered and reused following separation, maintaining their performance over multiple cycles and confirming their stability and economic feasibility for repeated microalgae harvesting and environmental applications [70,72–74].

4. Conclusion

This study demonstrated that *A. platensis* cultivation supplemented with carbon-coated iron-based nanoparticles offers a promising strategy for enhancing CO_2 capture, microalgal growth, and phycocyanin production. Among the two commercial nanoparticles tested, CALPECH NPs at a concentration of 100 $mg{\cdot}L^{-1}$ proved to be the most effective, likely due to their chemical composition, which contributed to a more efficient CO_2 uptake and pigment synthesis. Nanoparticle supplementation boosted biomass productivity up to 1.06 $g{\cdot}L^{-1}{\cdot}d^{-1}$ and phycocyanin content up to 178 $mg{\cdot}g^{-1}$, under high light intensity (600 $\mu mol{\cdot}m^{-2}{\cdot}s^{-1}$). In contrast, increasing light intensity from 300 to 600 $\mu mol{\cdot}m^{-2}{\cdot}s^{-1}$ led to a 42 % reduction in photosynthetic efficiency, likely due to photooxidative stress. NaCl levels above 0.2 M also induced stress in *A. platensis*, leading to a reduced photosynthetic efficiency in the presence of NPs. Overall, carbon-coated iron-based nanoparticles demonstrated antioxidant and biostimulant effects on *A. platensis* cultures, representing a promising strategy to enhance CO_2 capture, microalgal productivity and high-value compounds production during photosynthetic biogas upgrading. These findings lay the groundwork for future pilot-scale applications targeting sustainable biogas upgrading through *A. platensis* cultivation.

CRediT authorship contribution statement

Chrysa Anagnostopoulou: Data curation, Investigation, Visualization, Writing – original draft. **Laura Vargas-Estrada:** Methodology, Writing – review & editing. **Panagiotis G. Kougias:** Writing – review & editing. **Raúl Muñoz:** Conceptualization, Methodology, Supervision, Writing – review & editing, Funding acquisition.

Declaration of Competing Interest

The authors declare that they have no known competing financial interests or personal relationships that could have appeared to influence the work reported in this paper.

Appendix A. Supporting information

Supplementary data associated with this article can be found in the online version at doi:10.1016/j.procbio.2026.01.004.

Data availability

Data will be made available on request.

References

[1] P. Marconi, L. Rosa, Role of biomethane to offset natural gas, Renew. Sustain. Energy Rev. 187 (2023), https://doi.org/10.1016/j.rser.2023.113697.
[2] U.N. Kemka, T.E. Ogbulie, K. Oguzie, C.O. Akalezi, E.E. Oguzie, W. Asamoah, O.R. C. Nlemolisa, Algae, a biological purification tool for biogas upgrade: a review, EQA 64 (2024) 33–47, https://doi.org/10.6092/issn.2281-4485/19915.
[3] D. Marín, A.A. Carmona-Martínez, S. Blanco, R. Lebrero, R. Muñoz, Innovative operational strategies in photosynthetic biogas upgrading in an outdoors pilot scale algal-bacterial photobioreactor, Chemosphere 264 (2021), https://doi.org/10.1016/j.chemosphere.2020.128470.
[4] E.G. Hoyos, R. Kuri, T. Toda, R. Muñoz, Innovative design and operational strategies to improve CO2 mass transfer during photosynthetic biogas upgrading, Bioresour. Technol. 391 (2024), https://doi.org/10.1016/j.biortech.2023.129955.
[5] L. Méndez, R. Muñoz, Enhancing microalgae-based bioremediation technologies with carbon-coated zero valent iron nanoparticles, Algal Res 79 (2024), https://doi.org/10.1016/j.algal.2024.103448.
[6] C. Ruiz Palomar, A. García Álvaro, R. Muñoz, C. Repáraz, M.F. Ortega, I. de Godos, Pre-Commercial Demonstration of a Photosynthetic Upgrading Plant: Investment and Operating Cost Analysis, Processes 12 (2024), https://doi.org/10.3390/pr12122794.
[7] I. Angelidaki, L. Treu, P. Tsapekos, G. Luo, S. Campanaro, H. Wenzel, P.G. Kougias, Biogas upgrading and utilization: Current status and perspectives, Biotechnol. Adv. 36 (2018) 452–466, https://doi.org/10.1016/j.biotechadv.2018.01.011.
[8] R. Chaiklahan, N. Chirasuwan, T. Srinorasing, S. Attasat, A. Nopharatana, B. Bunnag, Enhanced biomass and phycocyanin production of Arthrospira (Spirulina) platensis by a cultivation management strategy: Light intensity and cell concentration, Bioresour. Technol. 343 (2022), https://doi.org/10.1016/j.biortech.2021.126077.
[9] A. Bose, R. O'Shea, R. Lin, J.D. Murphy, Optimisation and performance prediction of photosynthetic biogas upgrading using a bubble column, Chem. Eng. J. 437 (2022), https://doi.org/10.1016/j.cej.2022.134988.
[10] S.F. Ahmed, M. Mofijur, K. Tarannum, A.T. Chowdhury, N. Rafa, S. Nuzhat, P. S. Kumar, D.V.N. Vo, E. Lichtfouse, T.M.I. Mahlia, Biogas upgrading, economy and utilization: a review, Environ. Chem. Lett. 19 (2021) 4137–4164, https://doi.org/10.1007/s10311-021-01292-x.
[11] S. Srinuanpan, B. Cheirsilp, M.A. Kassim, Oleaginous microalgae cultivation for biogas upgrading and phytoremediation of wastewater, in: Microalgae Cultivation for Biofuels Production, Elsevier, 2019, pp. 69–82, https://doi.org/10.1016/B978-0-12-817536-1.00005-9.
[12] E. Abdelsalam, M. Samer, Y.A. Attia, M.A. Abdel-Hadi, H.E. Hassan, Y. Badr, Influence of zero valent iron nanoparticles and magnetic iron oxide nanoparticles on biogas and methane production from anaerobic digestion of manure, Energy 120 (2017) 842–853, https://doi.org/10.1016/j.energy.2016.11.137.
[13] R. Kumar, R. Mangalapuri, M.H. Ahmadi, D.V.N. Vo, R. Solanki, P. Kumar, The role of nanotechnology on post-combustion CO2 absorption in process industries, Int. J. Low. Carbon Technol. 15 (2020) 361–367, https://doi.org/10.1093/IJLCT/CTAA002.
[14] E.G. Hoyos, G. Amo-Duodu, U. Gulsum Kiral, L. Vargas-Estrada, R. Lebrero, R. Muñoz, Influence of carbon-coated zero-valent iron-based nanoparticle concentration on continuous photosynthetic biogas upgrading, Fuel 356 (2024), https://doi.org/10.1016/j.fuel.2023.129610.
[15] L. Vargas-Estrada, E.G. Hoyos, P.J. Sebastian, R. Muñoz, Influence of mesoporous iron based nanoparticles on Chlorella sorokiniana metabolism during photosynthetic biogas upgrading, Fuel 333 (2023), https://doi.org/10.1016/j.fuel.2022.126362.
[16] L. Giannelli, G. Torzillo, Hydrogen production with the microalga Chlamydomonas reinhardtii grown in a compact tubular photobioreactor immersed in a scattering light nanoparticle suspension, Int J. Hydrog. Energy 37 (2012) 16951–16961, https://doi.org/10.1016/J.IJHYDENE.2012.08.103.
[17] Grand View Research, Phycocyanin Market Size, Share & Trends Analysis Report By Application, By Region, And Segment Forecasts, 2024–2030. [Online] Available at: ⟨https://www.grandviewresearch.com/industry-analysis/phycocyanin-market-report⟩, (2024). ⟨https://www.grandviewresearch.com/press-release/global-phycocyanin-market⟩ (accessed August 6, 2025).
[18] D. Pez Jaeschke, I. Rocha Teixeira, L. Damasceno Ferreira Marczak, G. Domeneghini Mercali, Phycocyanin from Spirulina: A review of extraction methods and stability, Food Res. Int. 143 (2021), https://doi.org/10.1016/j.foodres.2021.110314.
[19] E. Posadas, M.L. Serejo, S. Blanco, R. Pérez, P.A. García-Encina, R. Muñoz, Minimization of biomethane oxygen concentration during biogas upgrading in algal-bacterial photobioreactors, Algal Res 12 (2015) 221–229, https://doi.org/10.1016/j.algal.2015.09.002.

[20] APHA, Standard methods: For the examination of water and waste water, American Public Health Association, Washington, DC, 2017. https://doi.org/10.1016/0003-2697(90)90598-4.
[21] R.A. Soni, K. Sudhakar, R.S. Rana, Comparative study on the growth performance of Spirulina platensis on modifying culture media, Energy Rep. 5 (2019) 327–336, https://doi.org/10.1016/j.egyr.2019.02.009.
[22] A. Bennett, L. Bogorad, COMPLEMENTARY CHROMATIC ADAPTATION IN A FILAMENTOUS BLUE-GREEN ALGA, J. CELL Biol. 58 (1973) 419–435.
[23] J. Demsar, T. Curk, A. Erjavec, C. Gorup, T. Hocevar, M. Milutinovic, M. Mozina, M. Polajnar, M. Toplak, A. Staric, M. Stajdohar, L. Umek, L. Zagar, J. Zbontar, M. Zitnik, B. Zupan, Orange: Data Mining Toolbox in Python, J. Mach. Learn. Res. (2013) 2349–2353.
[24] L. Vargas-Estrada, E.G. Hoyos, L. Méndez, P.J. Sebastian, R. Muñoz, Boosting photosynthetic biogas upgrading via carbon-coated zero-valent iron nanoparticle addition: A pilot proof of concept study, Sustain Chem. Pharm. 31 (2023), https://doi.org/10.1016/j.scp.2022.100952.
[25] C. Jäger, T. Henning, R. Schlögl, O. Spillecke, Spectral properties of carbon black, J. Non Cryst. Solids 258 (1999) 161–179. ⟨www.elsevier.com/locate/jnoncrysol⟩.
[26] M. Olszowy, What is responsible for antioxidant properties of polyphenolic compounds from plants? Plant Physiol. Biochem. 144 (2019) 135–143, https://doi.org/10.1016/j.plaphy.2019.09.039.
[27] M.A. Toropkina, A.G. Ryumin, I.O. Kechaikina, S.N. Chukov, Effect of humic acids on the metabolism of Chlorella vulgaris in a model experiment, Eurasia Soil Sci. 50 (2017) 1294–1300, https://doi.org/10.1134/S1064229317110126.
[28] X. Zheng, Z. Xu, D. Zhao, Y. Luo, C. Lai, B. Huang, X. Pan, Double-dose responses of Scenedesmus capricornus microalgae exposed to humic acid, Sci. Total Environ. 806 (2022) 150547, https://doi.org/10.1016/j.scitotenv.2021.150547.
[29] M. Dejsungkranont, Y. Chisti, S. Sirisansaneeyakul, Simultaneous production of C-phycocyanin and extracellular polymeric substances by photoautotrophic cultures of Arthrospira platensis, J. Chem. Technol. Biotechnol. 92 (2017) 2709–2718, https://doi.org/10.1002/jctb.5293.
[30] R. Chaiklahan, N. Khonsarn, N. Chirasuwan, M. Ruengjitchatchawalya, B. Bunnag, M. Tanticharoen, Response Spirulina platensis C1 High. Temp. High. Light Intensity (2007).
[31] L. Rudi, L. Cepoi, T. Chiriac, S. Djur, Interactions Between Potentially Toxic Nanoparticles (Cu, CuO, ZnO, and TiO2) and the Cyanobacterium Arthrospira platensis: Biological Adaptations to Xenobiotics, Nanomaterials 15 (2025), https://doi.org/10.3390/nano15010046.
[32] X. Zheng, Z. Xu, D. Zhao, Y. Luo, C. Lai, B. Huang, X. Pan, Double-dose responses of Scenedesmus capricornus microalgae exposed to humic acid, Sci. Total Environ. 806 (2022), https://doi.org/10.1016/j.scitotenv.2021.150547.
[33] M. Tong, X. Li, Q. Luo, C. Yang, W. Lou, H. Liu, C. Du, L. Nie, Y. Zhong, Effects of humic acids on biotoxicity of tetracycline to microalgae Coelastrella sp, Algal Res 50 (2020), https://doi.org/10.1016/j.algal.2020.101962.
[34] L. Jiang, S. Yu, H. Chen, H. Pei, Enhanced phycocyanin production from Spirulina subsalsa via freshwater and marine cultivation with optimized light source and temperature, Bioresour. Technol. 378 (2023) 129009, https://doi.org/10.1016/j.biortech.2023.129009.
[35] M.M.S. Ismaiel, M.D. Piercey-Normore, C. Rampitsch, Proteomic analyses of the cyanobacterium Arthrospira (Spirulina) platensis under iron and salinity stress, Environ. Exp. Bot. 147 (2018) 63–74, https://doi.org/10.1016/j.envexpbot.2017.11.013.
[36] M. Akbarnezhad, M. Shamsaie Mehrgan, A. Kamali, M.Javaheri Baboli, Bioaccumulation of Fe+2 and its effects on growth and pigment content of Spirulina (Arthrospira platensis), AACL Bioflux 9 (2016) 227–238. ⟨https://www.researchgate.net/publication/298412442⟩.
[37] E. Kougia, E. Ioannou, V. Roussis, I. Tzovenis, I. Chentir, G. Markou, Iron (Fe) biofortification of Arthrospira platensis: Effects on growth, biochemical composition and in vitro iron bioaccessibility, Algal Res 70 (2023), https://doi.org/10.1016/j.algal.2023.103016.
[38] V. Andriopoulos, M. Kornaros, Microalgal Phenolics: Systematic Review with a Focus on Methodological Assessment and Meta-Analysis, Mar. Drugs 22 (2024), https://doi.org/10.3390/md22100460.
[39] P.M. Mullineaux, M. Exposito-Rodriguez, P.P. Laissue, N. Smirnoff, ROS-dependent signalling pathways in plants and algae exposed to high light: Comparisons with other eukaryotes, Free Radic. Biol. Med 122 (2018) 52–64, https://doi.org/10.1016/j.freeradbiomed.2018.01.033.
[40] A. Dehghanipour, H. Zamani, Interaction of Fe2O3 nanoparticles with marine microalga Chlorella sorokiniana: Analysis of growth, morphological changes and biochemical composition, Plant Physiol. Biochem. 207 (2024), https://doi.org/10.1016/j.plaphy.2024.108385.
[41] S.X.Tong Liang, S. Djearamane, A.C. Tanislaus Antony Dhanapal, L.S. Wong, Impact of silver nanoparticles on the nutritional properties of Arthrospira platensis, PeerJ 10 (2022), https://doi.org/10.7717/peerj.13972.
[42] L. Vargas-Estrada, S. Torres-Arellano, A. Longoria, D.M. Arias, P.U. Okoye, P. J. Sebastian, Role of nanoparticles on microalgal cultivation: A review, Fuel 280 (2020), https://doi.org/10.1016/j.fuel.2020.118598.
[43] Y. Maltsev, K. Maltseva, M. Kulikovskiy, S. Maltseva, Influence of light conditions on microalgae growth and content of lipids, carotenoids, and fatty acid composition, Biol. (Basel) 10 (2021), https://doi.org/10.3390/biology10101060.
[44] L. Yang, Q. Su, B. Si, Y. Zhang, Y. Zhang, H. Yang, X. Zhou, Enhancing bioenergy production with carbon capture of microalgae by ultraviolet spectrum conversion via graphene oxide quantum dots, Chem. Eng. J. 429 (2022), https://doi.org/10.1016/j.cej.2021.132230.
[45] M.S. Rana, S.K. Prajapati, Resolving the dilemma of iron bioavailability to microalgae for commercial sustenance, Algal Res 59 (2021), https://doi.org/10.1016/j.algal.2021.102458.
[46] S. Li, X. Li, S.H. Ho, How to enhance carbon capture by evolution of microalgal photosynthesis? Sep Purif. Technol. 291 (2022) https://doi.org/10.1016/j.seppur.2022.120951.
[47] J. Cheng, Y. Zhu, K. Li, H. Lu, Z. Shi, Calcinated MIL-100(Fe) as a CO2 adsorbent to promote biomass productivity of Arthrospira platensis cells, Sci. Total Environ. 699 (2020), https://doi.org/10.1016/j.scitotenv.2019.134375.
[48] X. Yuan, X. Gao, C. Liu, W. Liang, H. Xue, Z. Li, H. Jin, Application of Nanomaterials in the Production of Biomolecules in Microalgae: A Review, Mar. Drugs 21 (2023), https://doi.org/10.3390/md21110594.
[49] L. Vargas-Estrada, E.G. Hoyos, P.J. Sebastian, R. Muñoz, Elucidating the role of nanoparticles on photosynthetic biogas upgrading: Influence of biogas type, nanoparticle concentration and light source, Algal Res 68 (2022), https://doi.org/10.1016/j.algal.2022.102899.
[50] K. Schipper, F. Fortunati, P.C. Oostlander, M. Al Muraikhi, H.M.S.J. Al Jabri, R. H. Wijffels, M.J. Barbosa, Production of phycocyanin by Leptolyngbya sp. in desert environments, Algal Res 47 (2020), https://doi.org/10.1016/j.algal.2020.101875.
[51] Y. Xie, Y. Jin, X. Zeng, J. Chen, Y. Lu, K. Jing, Fed-batch strategy for enhancing cell growth and C-phycocyanin production of Arthrospira (Spirulina) platensis under phototrophic cultivation, Bioresour. Technol. 180 (2015) 281–287, https://doi.org/10.1016/j.biortech.2014.12.073.
[52] H. Mutawie, Growth Metab. Response Filam. cyanobacterium Spirulina platensis Salin. Stress Sodium chloride (2015). ⟨http://www.lifesciencesite.comhttp://www.lifesciencesite.com.8⟩.
[53] S. Fal, A. Aasfar, R. Rabie, A. Smouni, H.E.L. Arroussi, Salt induced oxidative stress alters physiological, biochemical and metabolomic responses of green microalga Chlamydomonas reinhardtii, Heliyon 8 (2022). https://doi.org/10.1016/j.heliyon.2022.e08811.
[54] N. Touzout, M. Ainas, M. Babaali, H. Moussa, A. Mihoub, I. Ahmad, A. Jamal, S. Danish, R. Ahmad, Y.H. Dewir, Á. Székely, Potential effect of non-nitrogen fixing cyanobacteria Spirulina platensis on growth promotion of wheat (Triticum aestivum L.) under salt stress, Sci. Rep. 15 (2025), https://doi.org/10.1038/s41598-025-14567-y.
[55] N.P. Russo, M. Ballotta, L. Usai, S. Torre, M. Giordano, G. Fais, M. Casula, D. Dessì, P. Nieri, E. Damergi, G.A. Lutzu, A. Concas, Mixotrophic Cultivation of Arthrospira platensis (Spirulina) under Salt Stress: Effect on Biomass Composition, FAME Profile and Phycocyanin Content, Mar. Drugs 22 (2024), https://doi.org/10.3390/md22090381.
[56] A. Singh, R. Bol, V. Lovynska, R.K. Singh, J.R. Sousa, K. Ghazaryan, Application of nanoparticles for salinity stress management and biofortification in wheat: a review of dual approaches and insights, Front Plant Sci. 16 (2025), https://doi.org/10.3389/fpls.2025.1592866.
[57] A.M. Pirzada, T. Anwar, W.A. Qureshi, H. Qureshi, E.H. Siddiqi, W. Zaman, W. Soufan, Salinity stress mitigation in wheat through synergistic application of ascorbic acid, nanoparticles and Salvadora oleoides extract, Sci. Rep. 14 (2024), https://doi.org/10.1038/s41598-024-76194-3.
[58] X. Wang, Y. Xie, Z. Zhou, R. Ruan, C. Zhou, Y. Cheng, Factors Influencing Phycocyanin Synthesis in Microalgae and Culture Strategies: Toward Efficient Production of Alternative Proteins, Sustain. (Switz.) 17 (2025), https://doi.org/10.3390/su17135962.
[59] G.E. Lakatos, K. Ranglová, J. Câmara Manoel, T. Grivalský, J. Masojídek, Photosynthetic monitoring techniques indicate maximum glycogen accumulation in nitrogen-limited Synechocystis sp. PCC 6803 culture, Algal Res 55 (2021), https://doi.org/10.1016/j.algal.2021.102271.
[60] A. Nath, P.K. Tiwari, A.K. Rai, S. Sundaram, Evaluation of carbon capture in competent microalgal consortium for enhanced biomass, lipid, and carbohydrate production, 3 Biotech 9 (2019), https://doi.org/10.1007/s13205-019-1910-6.
[61] K. Sujatha, P. Nagarajan, Effect of salinity on biomass and biochemical constituents of Spirulina platensis (Geitler), Nternat J. Plant 7 (2014) 71–73. ⟨www.researchjournal.co.in⟩.
[62] P.H. Ravelonandro, D.H. Ratianarivo, C. Joannis-cassan, Improv. Growth Arthrospira (Spirulina) platensis Toliara (Madag.) Eff. Agit. Salin. CO2 Addit. 89 (2011) 209–216, https://doi.org/10.1016/j.fbp.2010.04.009i.
[63] S. Fal, A. Aasfar, R. Rabie, A. Smouni, H.E.L. Arroussi, Salt induced oxidative stress alters physiological, biochemical and metabolomic responses of green microalga Chlamydomonas reinhardtii, Heliyon 8 (2022). https://doi.org/10.1016/j.heliyon.2022.e08811.
[64] T. Uzlasir, O. Isik, L.H. Uslu, S. Selli, H. Kelebek, Impact of different salt concentrations on growth, biochemical composition and nutrition quality of Phaeodactylum tricornutum and Spirulina platensis, Food Chem. 429 (2023), https://doi.org/10.1016/j.foodchem.2023.136843.
[65] A. Macías-de la Rosa, L. López-Rosales, A. Contreras-Gómez, A. Sánchez-Mirón, F. García-Camacho, M.D.C. Cerón-García, Salinity as an Abiotic Stressor for Eliciting Bioactive Compounds in Marine Microalgae, Toxins (Basel) 16 (2024), https://doi.org/10.3390/toxins16100425.
[66] G. Markou, E. Kougia, D. Arapoglou, I. Chentir, V. Andreou, I. Tzovenis, Production of Arthrospira platensis: Effects on Growth and Biochemical Composition of Long-Term Acclimatization at Different Salinities, Bioengineering 10 (2023), https://doi.org/10.3390/bioengineering10020233.
[67] P. Shetty, M.M. Gitau, G. Maróti, Salinity stress responses and adaptation mechanisms in eukaryotic green microalgae, Cells 8 (2019), https://doi.org/10.3390/cells8121657.
[68] K.M. Singh, A.B. Jha, R.S. Dubey, P. Sharma, Nanoparticle-mediated mitigation of salt stress-induced oxidative damage in plants: insights into signaling, gene

expression, and antioxidant mechanisms, Environ. Sci. Nano (2025), https://doi.org/10.1039/D5EN00174A.
[69] L. Moraes, G.M. da Rosa, M. da, R.A.Z. de Souza, J.A.V. Costa, Carbon dioxide biofixation and production of spirulina sp. LEB 18 biomass with different concentrations of NaNO3 and NaCl, Braz. Arch. Biol. Technol. 61 (2018), https://doi.org/10.1590/1678-4324-2018150711.
[70] P. Fraga-García, P. Kubbutat, M. Brammen, S. Schwaminger, S. Berensmeier, Bare iron oxide nanoparticles for magnetic harvesting of microalgae: From interaction behavior to process realization, Nanomaterials 8 (2018), https://doi.org/10.3390/nano8050292.
[71] F. Almomani, Algal cells harvesting using cost-effective magnetic nano-particles, Sci. Total Environ. 720 (2020), https://doi.org/10.1016/j.scitotenv.2020.137621.
[72] Y.C. Lee, K. Lee, Y.K. Oh, Recent nanoparticle engineering advances in microalgal cultivation and harvesting processes of biodiesel production: A review, Bioresour. Technol. 184 (2015) 63–72, https://doi.org/10.1016/j.biortech.2014.10.145.
[73] A. Abo Markeb, J. Llimós-Turet, I. Ferrer, P. Blánquez, A. Alonso, A. Sánchez, J. Moral-Vico, X. Font, The use of magnetic iron oxide based nanoparticles to improve microalgae harvesting in real wastewater, Water Res 159 (2019) 490–500, https://doi.org/10.1016/j.watres.2019.05.023.
[74] S. Sinha, R. Sharma, M.R. Ansari, R. Singh, S. Pathak, N. Jahan, K.R. Peta, Multifunctional oleic acid functionalized iron oxide nanoparticles for antibacterial and dye degradation applications with magnetic recycling, Mater. Adv. 6 (2025) 2253–2268, https://doi.org/10.1039/d5ma00036j.